An Open-Source Ultrasound Software for Diagnosis of Fistula Maturation

Barry Belmont,* Dae Woo Park,† William F. Weitzel,‡§ and Albert J. Shih*†

Vascular access is essential for hemodialysis patients. The mature native arteriovenous fistula has been the preferred vascular access for hemodialysis, because it has greater longevity than synthetic grafts. However, once surgically created, fistulas often fail to develop (mature) into viable points of vascular access, requiring surgical or radiologic interventions before their use. Because maturation depends on vascular mechanics (*e.g.,* distensibility and wall shear), we developed open-source ultrasound software to investigate these metrics clinically. We demonstrated in a single patient the ability of the software for consistent measurements from various locations within a cardiac cycle and between different cardiac cycles. We further assessed the ability of the software to identify changes in distensibility of a patient's fistula from 1 to 6 weeks postoperation. The routine frame rates of clinical machines demonstrated high fidelity tracking within cardiac cycles (coefficient of variation [CV] = 2.4% ± 0.011) and between cardiac cycles (CV = 2.4% ± 0.004). The distensibility of the patient's fistula from 1 to 6 weeks postoperation increased from 4% to 7% in the arterial inflow and from 3% to 4% in the postarterial anastomotic segment (PAAS). In contrast, the distensibility of the outflow vein decreased from 4% to 2%. These results corroborate that in addition to diameter changes, the mechanical properties of the vascular segments changed during fistula maturation. This demonstrates that our software-based approach may allow ultrasound-based mechanical measurements to become more accessible for wider clinical research. *ASAIO Journal* 2018; 64:70–76.

Key Words: autogenous arteriovenous fistulas, distensibility, flow gradient

Vascular access is a lifeline for hemodialysis patients whose treatment requires consistent and reliable access to their bloodstream. Determining an optimal method to achieve long-term, consistent vascular access of hemodialysis continues to poses unique challenges for caregivers as the complex interplay of clinical treatment and mechanical response is not yet fully understood. Three main types of vascular access are as follows: 1) a catheter—usually made of polyurethane and silicone[1] and inserted into a central vein often used to initiate dialysis although more permanent access (graft or fistula) is established; 2) a graft—a prosthetic tube often made of polytetrafluorethylene that connects an artery to a vein; and 3) a arteriovenous (AV) fistula—a surgically created connection of an artery to a vein using the patients' autogenous vessels. In all cases, the goal is to enable the local vascular environment to withstand large volumes of fluid exchange, such as by facilitating the cannulation of large bore needles used in hemodialysis. Although both grafts and fistulas are designed for long-term use, current guidelines recommend autogenous AV fistulas as the preferred mode of vascular access for patients undergoing hemodialysis.[2–4] Fistulas, however, often fail to mature at alarming rates (from 10% to 70%).[3–7] Such failure interrupts life-sustaining dialysis treatments, often leading to procedures and sometimes hospitalizations for surgical revision or new fistula creation, adding to the overall cost of care, increasing the medical risks, and causing unnecessary stress to the patients.

Ideally, clinicians need to determine fistula development to monitor outpatients and modify as necessary to help with maturation and maintenance.[8] To determine the fistula development, clinicians measure mechanical properties of the surgically created vasculature—such as the diameters, the distensibility, and the volumetric flows of the inflow artery, the outflow vein, and the postarterial anastomotic segment (PAAS)[9–12]—as these are critical for AV fistula maturation. As the local arterial environment begins to interact with the local venous environment, many changes are expected to occur including the desired dilation of the outflow vein as a result of the increased pressure and fluid flow associated with the arterial system. Ultimately, the vasculature is shaped by the forces within as these are mechanotransduction in the vessels, prompting the release of chemical factors (such as nitric oxide) that promote vessel modification (such as vasodilation of wall thickening). Several studies have shown myriad mechanical properties affect, and help predict, fistula maturation.[9–12] For example, low arterial elasticity has been associated with stenosis and failure,[13] increased venous distensibility has been associated with maturation and patency,[11] and vein diameter alone has proven an effective predictor of successful fistulas.[14] Ultrasound has been utilized to assess the anatomical, physiologic, and mechanical feedback system regulating the patency of fistulas. Currently, no clinically applicable diagnostic system exists to measure these parameters.

Previous research has demonstrated the feasibility of measuring vascular elasticity using radiofrequency (RF) data.[15,16] However, clinicians are limited to access the RF data in clinical ultrasound machines. Instead, most clinical ultrasound machines provide the digital imaging and communications in medicine (DICOM) data. Although DICOM data have less spatial resolution than RF data, their spatial resolution is sufficient to identify

From the *Biomedical Engineering, University of Michigan, Ann Arbor, Michigan; †Innovative Medical Engineering and Technology, National Cancer Center, Goyang-si, Gyeonggi-do, Republic of Korea; ‡Veterans Affairs Ann Arbor Health System, Ann Arbor, Michigan; and §Internal Medicine, Ann Arbor, Michigan.

Submitted for consideration December 2016; accepted for publication in revised form April 2017.

Disclosures: The authors have no conflicts of interest to report.

This work was supported in part by NIH grant R21DK100753.

Correspondence: Dae Woo Park, Innovative Medical Engineering and Technology, National Cancer Center, 323 Ilsan-ro, Ilsandong-gu, Goyang-si, Gyeonggi-do, 10408, Republic of Korea. Email: bigrain@ncc.re.kr.

DOI: 10.1097/MAT.0000000000000590

the vessel wall motion. For example, DICOM-based videos have been used to measure the elasticity of carotid arteries.[17]

The goal of this study was to develop and test the performance of a software we developed to measure the vascular distensibility, strain, and flow gradient near the vessel wall of a patient's fistulas using rigorous ultrasound speckle tracking methods. The software, designed for clinical researchers, uses ultrasound DICOM data collected in clinic to evaluate fistula maturation by noninvasively measuring vascular distensibility, strain, and flow gradients. The software was validated by testing its ability to track ultrasound data from a subject immediately (1 week) after fistula creation and at 6 weeks follow-up. This is as part of a larger goal to make this ultrasound software tool openly available to study the likelihood of success or failure of AV fistulas. An overview of the software itself, the feature tracking algorithm underlying it, and its initial clinical evaluation are presented.

Overview of the Software

The software was designed and implemented in MATLAB (v. 2016a; Mathworks, Natick, MA) and comprised a graphical user interface (GUI). **Figure 1** shows the GUI and four main functions of the software that include: (1) image adjustment, (2) saving and loading images, (3) image analysis, and (4) selecting region of interest (ROI). In function (1), users can manually adjust images such as (a) altering the color histogram of image, (b) changing the brightness and contrast parameters, (c) zooming into and out of an image (including a zoom-to-fit function), (d) overlaying a grid on the present image for quick estimations, and (e) selecting a colormap to aid in visualization and presentation. In function (2), users can import or export images and edit or save image frames including (f) saving the present image, (g) saving a single frame or a stack of frames, (h) editing or exporting data, and (i) importing a new image. Function (3) allows users to filter DICOM images and analyze data by (k) filtering using either a median or Kalman filter (l) setting up the calibrating parameters, and (m) analyzing the pulsatility, strain (either total image or specific vessel wall), and overall decorrelation of images. Function (4) presents users with the option to specify one or more regions of interest (ROIs) in the image, and (p) calculate the mean and standard deviation of the pixels within those one or more ROIs. Furthermore, function 4 allows (n) selecting an ROI and (o) deleting or exporting an ROI. The software also has display functions, wherein (j) the current frame and the total frame numbers are presented, (q) the pixel intensity values at the cursor are shown, and (r) each of the video frame by frame can be scrolled either using a scroll bar or a mouse wheel.

This software allows investigators to evaluate three key mechanical parameters: 1) distensibility—tracking vessel diameter changes over time; 2) strain—measuring deformation with reference to a desired geometry; and 3) flow gradient—computing the decorrelation caused by a fluid flow over a certain amount of time. These three parameters have been measured by previous investigators to determine vascular mechanics.[15–18]

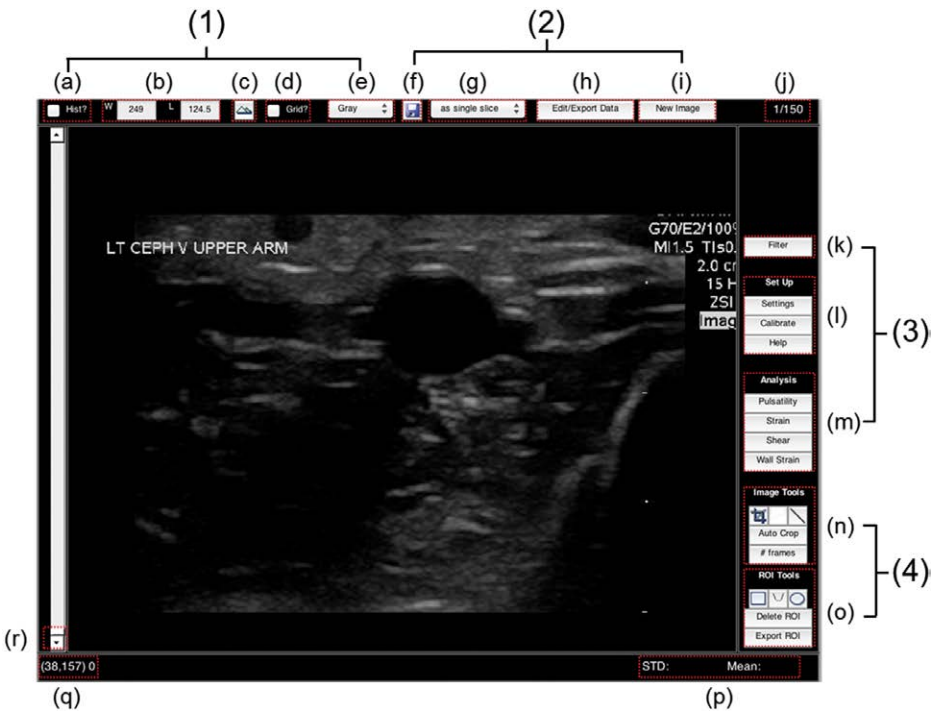

Figure 1. The main GUI and four main functions: (1) image adjustment, (2) save and load images, (3) image analysis, and (4) selecting ROI. Function (1), manual adjustment of images: (a) color histogram of image, (b) brightness and contrast parameters, (c) a zoom-to-fit function, (d) overlaying a grid, and (e) the color map selection. Function (2), users can import or export images and edit or save image frames: (f) save image, (g) a single frame or the entire video, (h) the edit or export data, and (i) importing a new image. Function (3), users can filter DICOM images and analyze data: (k) filter (median or Kalman filter), (l) setting up the image, (m) analyzing the pulsatility, strain (either total image or specific vessel wall), and decorrelation of images. Function (4), users can specify ROI in the image and calculate mean and standard deviations within the ROI: (n) selecting ROI, (o) deleting or exporting ROI, and (p) calculating the mean and standard deviation of the pixels within the ROIs. Display function: (j) the current frame and the total frame numbers, (q) the pixel intensity values at the cursor, and (r) scrolling through each of the video frame by frame. DICOM, digital imaging and communications in medicine; GUI, graphical user interface; ROI, region of interest.

Our purpose was to measure these three parameters to predict AV fistula maturation through semiautomated digital image correlation methods.

Feature Tracking Algorithm

Two techniques were utilized for tracking algorithm: the Kanade-Lucas-Tomasi (KLT) feature tracker and pyramidal segmentation. The KLT feature tracker utilizes spatial intensity gradients to track the displacement of features within an image across consecutive frames. However, KLT feature tracking relies on small displacements of features from frame-to-frame, and hence the identification of large motion vectors such as vessel dilation during each cardiac cycle is limited. To measure such large motion vectors, our algorithm employs a pyramidal segmentation technique to subsample an image, reducing its resolution, and increasing the spatial information inherent in each pixel to perform large motion tracking, and then feeding the displacement results found from the low-resolution images to high-resolution images. Eventually, the accuracy and speed of tracking can be achieved using the KLT technique with pyramidal segmentation.

Figure 2, **A** and **B** demonstrates the pyramidal segmentation process utilized in our software. **Figure 2A** illustrates an image pyramid of an ultrasound image of a patient's PAAS created via subsampling, and **Figure 2B** shows how the image pyramid

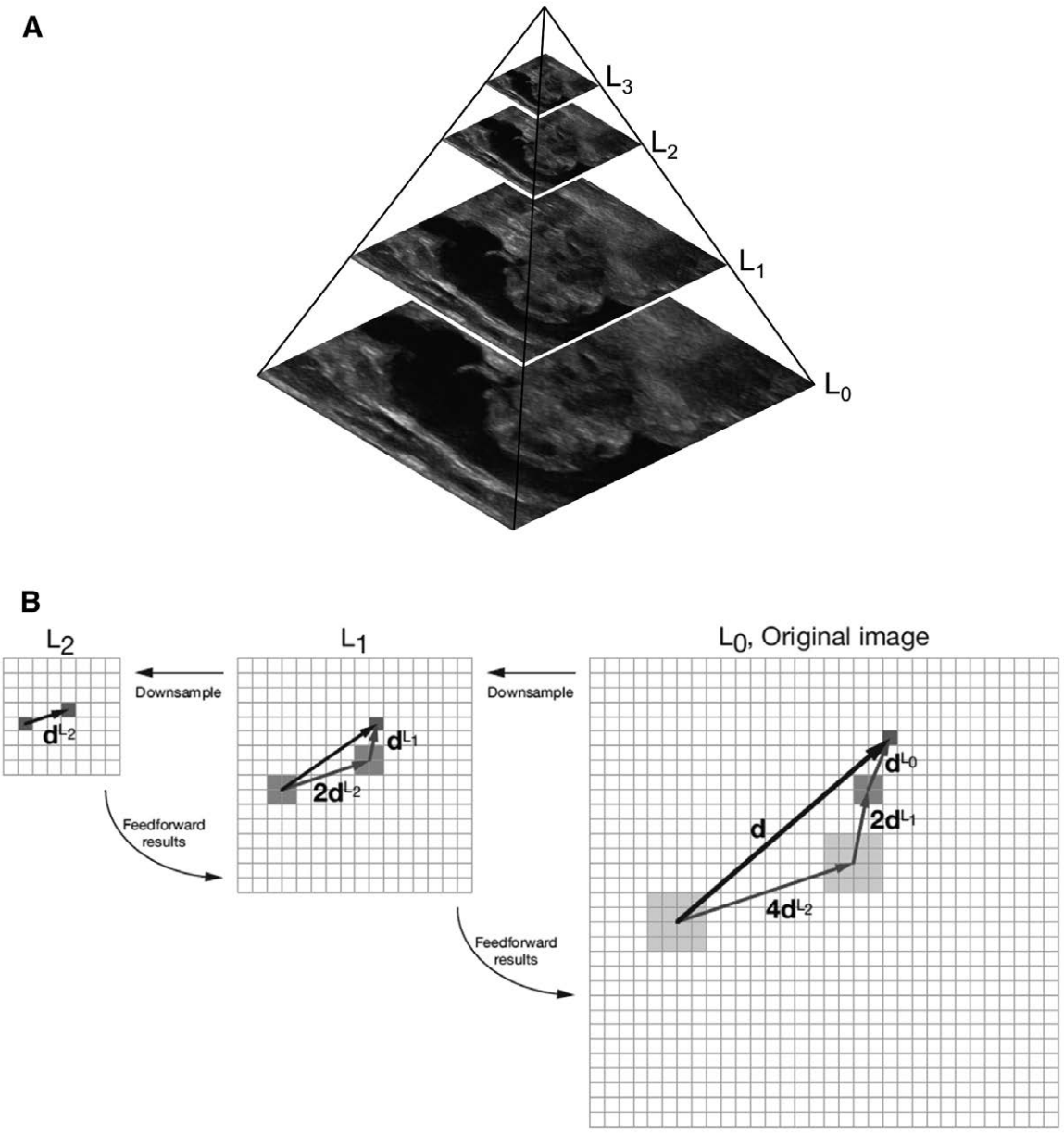

Figure 2. An example of the iterative process used to track a feature across a pyramidal segment image: (**A**) image pyramid of an ultrasound image of a patient's PAAS created by subsampling segmentation and (**B**) the iterative process for feature tracking. PAAS, postarterial anastomotic segment.

is used in the iterative process of feature tracking. The lowest subsampled image is used for an initial motion estimation using the KLT algorithm. A displacement vector, computed at one level, is fed to the below level (*i.e.,* to a higher resolution image), where the KLT algorithm is again performed using the displacement information from the previous level as its starting point. The process is continued until tracking is performed on the highest resolution image (the original image, the bottom of the pyramid).

More specifically, starting with an image of resolution $W \times H$ at a level L_0, an image pyramid is built by subsampling the image at each level, in this case by a factor of 2 along each coordinate direction. An initial displacement at that level (m), d^{L_m}, is computed at the uppermost pyramid level by minimizing its level-specific residual function of the form

$$\varepsilon^{L_m}\left(d^{L_m}\right) = \sum_{x=u_x^L-w_x}^{u_x^L+w_x} \sum_{x=u_y^L-w_y}^{u_y^L+w_y} \left[I_1^L(x,y) - I_2^L\left(x+d_x^L+g_x^L, y+d_y^L+g_y^L\right)\right]^2 \quad (1)$$

where ε is the residual error, L_m represents the level m being evaluated, d^{L_m} is the displacement vector, w_x and w_y are the window size parameters of the images I_1^L and I_2^L each with a window size equal to $(2w_x+1)\times(2w_y+1)$ centered at a point (x,y), u_x^L and u_y^L represent specific pixel values within the images, and g_x^L and g_y^L are displacement estimations fed through from the level above (at the highest level, the estimation is 0). The displacement d^{L_m} is passed as the initial guess, g_x^L and g_y^L, down to the next pyramidal image level, L_{m-1}, to find a value of $d^{L_{m-1}}$ that minimizes its residuals at specific level. This process is continued until the final image at level L_0 is reached, from which a final motion vector, $d = d^{L_0}$, is calculated.

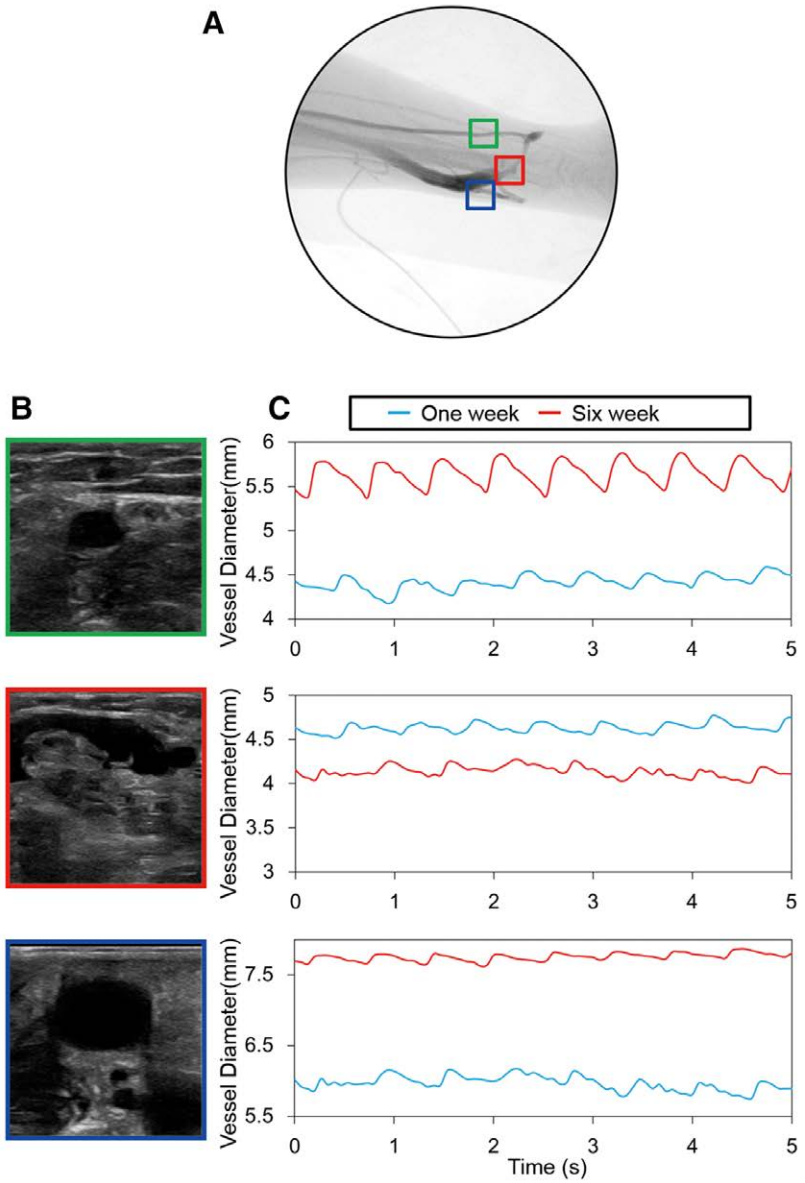

Figure 3. An example of vessel diameter *vs.* time measured in the artery, PAAS, and vein from a patient: (**A**) the fistulogram, (**B**) B-mode images of the artery (green box), PAAS (red box), and vein (blue box), and (**C**) the diameter as a function of time over several cardiac cycles measured at 1 week postoperatively and 6 weeks postoperatively. PAAS, postarterial anastomotic segment. full color online

Distensibility

To measure the distensibility of a vessel, users are prompted to select two points of interest. These two points are tracked using the KLT feature tracking algorithm[19] based on the MATLAB image processing toolbox. The distance between the two points is computed over the entire stack of images (usually in the form of a video or a "cine loop"), and a graph of the distensibility over time is presented in the GUI. The distensibility can be displayed as a measure of absolute distance, relative distance, normalized as a percent of the maximum value, and normalized as a percent of the minimum value. The software also allows the user to select multiple paired points to examine the relationship between several points along a vessel simultaneously. **Figure 3A** shows a subject's fistulogram; **Figure 3B** shows B-mode images of the artery (green box), the PAAS (red box), and the vein (blue box); and **Figure 3C** illustrates the vessel diameter as a function of time over several cardiac cycles measured from a patient's inflow artery, PAAS, and outflow vein at 1 week postoperatively and 6 weeks postoperatively. The blue solid line and red solid line of the graphs presented in **Figure 3C** represent 1 and 6 week postoperation, respectively, for a patient. Based on the relative motion of the points, the vessel distensibility is calculated and displayed over the acquisition period.

Strain

The software enables users to measure the relative and absolute changes in the distance between pixels of the image over time in an ROI. That is, users can determine strain in two distinct ways: frame-to-frame strain or cumulative strain (*e.g.,* over a cardiac cycle). For both strains, users can select a fraction of pixels (ranging for 1–100% in increments of 1%) to track within an ROI for strain computation. The lateral strain (across the ultrasound beam direction), axial strain (along the ultrasound beam direction), and the overall magnitude of the strain are calculated by the software and can be saved as a strain map. The equations of lateral strain (ε_L), axial strain (ε_A), and the magnitude of strain (ε) used by the software are as follows:

$$\varepsilon_L = \frac{\partial u_L}{\partial L},\ \varepsilon_A = \frac{\partial u_A}{\partial A} \text{ and } \varepsilon = \sqrt{\varepsilon_L^2 + \varepsilon_A^2} \tag{2}$$

where du_L and du_A are the measured displacements, and dL and dA are the initial lengths in lateral and axial directions, respectively. **Figure 4** shows an example of a strain magnitude map of a draining cephalic vein accumulated over a single cardiac cycle.

Flow Gradient

Flow gradients near the vessel walls can be measured by users using the speckle decorrelation.[16,18] The speckle decorrelation computes the scatterers motion in frame-to-frame. As scatterers pass across the ultrasound beam, the correlation of the current image to an initial reference frame decreases as a function of scatterers displacement. In other words, the amount of speckle decorrelation is indicative of the rate of scatterers flowing through the imaging beam.

In the software, users are prompted to select two points of interest (preferably a vessel edge and a point toward the center of the vessel), and the flow gradient is found between two points. The flow gradient can be transformed into the wall shear rate using a correlation versus speckle displacement calibration curve.[18] The wall shear rate ($\frac{\partial v}{\partial r}$) is calculated by dividing the flow speed (dv) by the distance from the wall edge (dr). Users can input a correlation versus speckle displacement curve as functional parameters in the software.

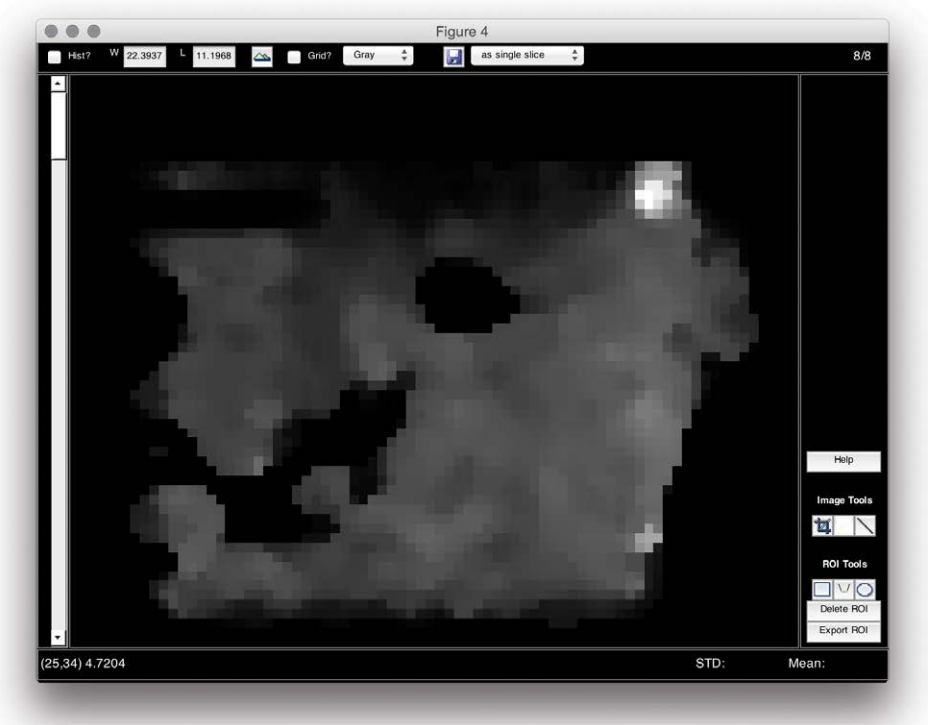

Figure 4. A strain magnitude map of a cephalic vein accumulated over a single cardiac cycle.

Figure 5 demonstrates the results of a flow gradient measurement at the vessel edge compared with an ideal Poiseuille velocity curve calculated from vessel diameter and the Doppler volumetric flow measurement for the same location of a patient. The flow gradient was calculated by fitting a line using a least square linear regression across the first three velocity points from the edge.

Clinical Evaluation

A subject was enrolled after providing informed consent under our local Institutional Review Board approval. The subject was a 68-year-old male, and standard DICOM cine loop data were collected from the subject's left brachiocephalic fistula at 1 and 6 weeks postsurgical creations. His comorbidities were hypertension, coronary artery disease, and peripheral vascular disease. The ultrasound images were acquired by a sonographer using a clinical ultrasound probe for long and short axes of the arterial inflow (10 cm upstream from the PAAS), the PAAS, and the venous outflow (10 cm downstream from the PAAS). Six seconds of cine loop data were collected at frame rate 15 Hz, using a ZS3 ultrasound system (Zonare, Mountain View, CA) with a 7 MHz probe.

The vessel distensibility was calculated using the software to determine the intracardiac and intercardiac variability: a first test measuring various locations within a cardiac cycle and a second test measuring between different cardiac cycles. **Figure 6**, **A** and **B** show the bar graphs of vessel distensibility for the artery, the PAAS, and the vein determined from these first and second tests, respectively. **Figure 6A** shows the coefficient of variation to be very small for all vessels across all analyses (three vessels on two independent measurements). **Figure 6B** shows consistent intercardiac measurements between cardiac cycles. Note that the intracardiac cycle measurement variation is less than the intercardiac cycle variation, suggesting that there is some beat-to-beat variation in the vascular strain perhaps because of fluctuations in stroke volume or beat-to-beat blood pressure changes.

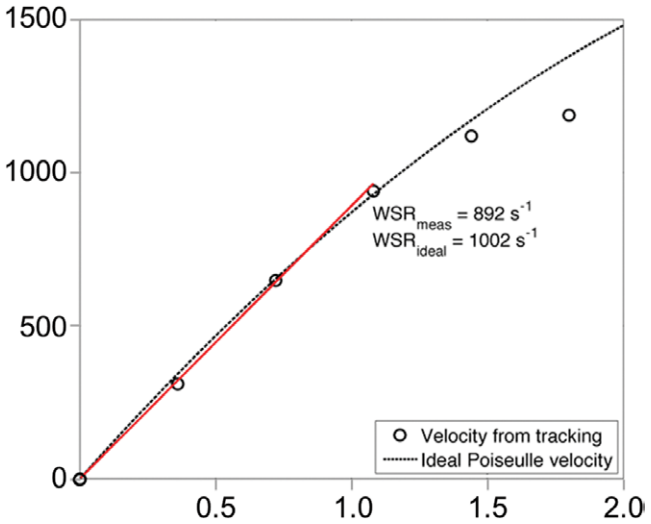

Figure 5. Blood velocity profile in a brachial artery obtained by decorrelation measurements and modeled from an ideal Poiseuille flow. full color online

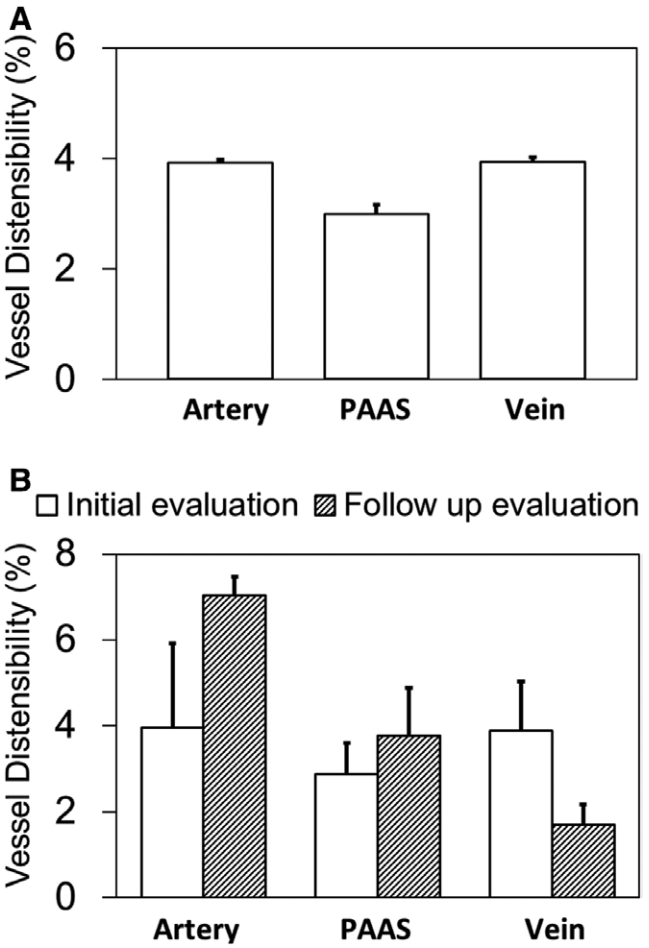

Figure 6. The bar graphs of vessel distensibility for a patient's artery, PAAS, and vein. **A**: The vessel distensibility measured from various locations within a cardiac cycle and (**B**) the vessel distensibility determined between different cardiac cycles on a patient at 1 week postoperatively (initial evaluation) and 6 weeks postoperatively (follow-up evaluation). PAAS, postarterial anastomotic segment.

Conclusions and Future Work

We have taken the first major step to develop robust software to measure the mechanical parameters using standard DICOM data. The software demonstrated the capacity to compute frame-to-frame displacement and strain, yielding automated measurements of distensibility throughout sequential cardiac cycles. The results suggest these measurements are robust and repeatable from DICOM data within individual cardiac cycles and between successive cardiac cycles. The decorrelation gradients, related to wall shear, were attainable in this case and show promise, but are highly dependent on the frame rate and velocity gradient at the vessel wall. Further clinical testing and analysis will be required to determine the reliability and limitations of both of these measurements.

Although this software is based on the proprietary MATLAB package, MATLAB is available at many academic institutions and research facilities. We made these MATALB libraries available on GitHub, San Francisco, California, USA in efforts to build collaboration in advancing this methodology and encouraging widespread clinical study. We are also exploring Python, Python Software Foundation, Wilmington, Delaware, USA or

other distributions that will increase the accessibility of this methodology for research. We have also made this software open source to improve collaborative research in ultrasound-based vascular mechanics.

In this study, the subject's access matured (dilated sufficiently) for dialysis access. Although we should not overreach in correlating the measurements with outcomes using data from a single patient, these data demonstrate the increase in distensibility of the artery consistent with healthy remodeling as the artery dilates during maturation. In addition, the decrease in vein wall distensibilty was seen as expected with vascular wall remodeling as the vein diameter increased during healthy maturation. The data also show the feasibility of performing these measurements in future studies to assess the correlation of these measurements with clinical outcomes.

The larger clinical research goal is to stimulate more research to help to determine factors that will improve dialysis fistula maturation. More broadly, this software was designed for clinical researchers to use standard ultrasound images commonly collected in routine vascular clinic evaluations for any peripheral vascular evaluation. Because the process is based entirely on robust speckle tracking methodology and postprocessing of standard ultrasound DICOM cine loop data, there is great opportunity for research investigators to improve vascular diagnostics using this methodology.

The most current working version of the software is located at https://github.com/WuMRC/fistula.

References

1. Tal MG, Ni N: Selecting optimal hemodialysis catheters: Material, design, advanced features, and preferences. *Tech Vasc Interv Radiol* 11: 186–191, 2008.
2. National Kidney Foundation: K/DOQI clinical practice guidelines and clinical practice recommendations for diabetes and chronic kidney disease. *Am J Kidney Dis* 49 (suppl 2): S1–S180, 2007.
3. Rayner HC, Besarab A, Brown WW, Disney A, Saito A, Pisoni RL: Vascular access results from the Dialysis Outcomes and Practice Patterns Study (DOPPS): Performance against Kidney Disease Outcomes Quality Initiative (K/DOQI) Clinical Practice Guidelines. *Am J Kidney Dis* 44 (5 suppl 2): 22–26, 2004.
4. Ethier J, Mendelssohn DC, Elder SJ, *et al*: Vascular access use and outcomes: An international perspective from the Dialysis Outcomes and Practice Patterns Study. *Nephrol Dial Transplant* 23: 3219–3226, 2008.
5. Patel ST, Hughes J, Mills JL Sr: Failure of arteriovenous fistula maturation: An unintended consequence of exceeding dialysis outcome quality initiative guidelines for hemodialysis access. *J Vasc Surg* 38: 439–445, 2003; discussion 445.
6. Gibson KD, Gillen DL, Caps MT, Kohler TR, Sherrard DJ, Stehman-Breen CO: Vascular access survival and incidence of revisions: A comparison of prosthetic grafts, simple autogenous fistulas, and venous transposition fistulas from the United States Renal Data System Dialysis Morbidity and Mortality Study. *J Vasc Surg* 34: 694–700, 2001.
7. Lok CE, Sontrop JM, Tomlinson G, *et al*: Cumulative patency of contemporary fistulas versus grafts (2000–2010). *Clin J Am Soc Nephrol* 8: 810–818, 2013.
8. Berman SS, Gentile AT: Impact of secondary procedures in autogenous arteriovenous fistula maturation and maintenance. *J Vasc Surg* 34: 866–871, 2001.
9. Parmar J, Aslam M, Standfield N: Pre-operative radial arterial diameter predicts early failure of arteriovenous fistula (AVF) for haemodialysis. *Eur J Vasc Endovasc Surg* 33: 113–115, 2007.
10. Mendes RR, Farber MA, Marston WA, Dinwiddie LC, Keagy BA, Burnham SJ: Prediction of wrist arteriovenous fistula maturation with preoperative vein mapping with ultrasonography. *J Vasc Surg* 36: 460–463, 2002.
11. van der Linden J, Lameris TW, van den Meiracker AH, de Smet AA, Blankestijn PJ, van den Dorpel MA: Forearm venous distensibility predicts successful arteriovenous fistula. *Am J Kidney Dis* 47: 1013–1019, 2006.
12. Huber TS, Ozaki CK, Flynn TC, *et al*: Prospective validation of an algorithm to maximize native arteriovenous fistulae for chronic hemodialysis access. *J Vasc Surg* 36: 452–459, 2002.
13. Kheda MF, Brenner LE, Patel MJ, *et al*: Influence of arterial elasticity and vessel dilatation on arteriovenous fistula maturation: A prospective cohort study. *Nephrol Dial Transplant* 25: 525–531, 2010.
14. Lauvao LS, Ihnat DM, Goshima KR, Chavez L, Gruessner AC, Mills JL Sr: Vein diameter is the major predictor of fistula maturation. *J Vasc Surg* 49: 1499–1504, 2009.
15. Weitzel WF, Kim K, Henke PK, Rubin JM: High-resolution ultrasound speckle tracking may detect vascular mechanical wall changes in peripheral artery bypass vein grafts. *Ann Vasc Surg* 23: 201–206, 2009.
16. Park DW, Kruger GH, Rubin JM, *et al*: *In vivo* vascular wall shear rate and circumferential strain of renal disease patients. *Ultrasound Med Biol* 39: 241–252, 2013.
17. Yli-Ollila H, Laitinen T, Weckström M, Laitinen TM: Axial and radial waveforms in common carotid artery: An advanced method for studying arterial elastic properties in ultrasound imaging. *Ultrasound Med Biol* 39: 1168–1177, 2013.
18. Park DW, Kruger GH, Rubin JM, *et al*: Quantification of ultrasound correlation-based flow velocity mapping and edge velocity gradient measurement. *J Ultrasound Med* 32: 1815–1830, 2013.
19. Lucas BD, Kanade T: *An Iterative Image Registration Technique With an Application to Stereo Vision. Proceedings of the 7th International Joint Conference on Artificial Intelligence*. San Francisco, CA, Morgan Kaufmann Publishers Inc,1981, p. 674–679.